Springer

KSME

Journal of Mechanical Science and Technology 30 (2) (2016) 943~952
www.springerlink.com/content/1738-494x(Print)/1976-3824(Online)
DOI 10.1007/s12206-016-0148-z

Experimental investigation of forced convective heat transfer enhancement of γ-Al_2O_3/water nanofluid in a tube †

Aminreza Noghrehabadi* and Rashid Pourrajab

Department of Mechanical Engineering, Shahid Chamran University of Ahvaz, Ahvaz, Iran

(Manuscript Received May 31, 2015; Revised September 2, 2015; Accepted October 11, 2015)

Abstract

The effect of nanofluids on heat transfer inside circular tubes under uniform constant heat flux boundary condition was investigated. The working nanofluid was a suspension of γ-Al_2O_3 nanoparticles of average diameter 20 nm. The heat transfer coefficients were calculated experimentally in the range of $1057 < Re < 2070$ with different particle volume concentrations of 0.1%, 0.3% and 0.9%. Increasing the particle volume fraction led to enhancement of the convective heat transfer coefficient. The results show that the average heat transfer coefficient increased 16.8% at 0.9% volume concentration and Reynolds number of 2070 compared with distilled water. In addition, the enhancement of the convective heat transfer was particularly significant in the entrance region and decreased with axial distance. Finally, an empirical correlation for Nusselt number has been proposed for the present range of nanofluids. The mean deviation between the predicted Nusselt number and experimental values for the new correlation is 3.57%.

Keywords: Alumina nanofluid; Convective heat transfer; Circular tube; Thermal developing region; Correlation

1. Introduction

The increasing need for enhanced heat transfer rates is driven by the development of smaller instruments with very high heat flux rates. The thermal management of these instruments requires systems that are more helpful in removing heat. The revolutionary advances in thermal management have resulted in the ability to incorporate the latest advances in technology. Many efforts have been made to improve the design of heat exchangers. However, the design improvements of heat exchangers can make only partial improvements in heat removal rates; so other ways such as alternate fluids or higher conductivity solids are needed to access greater steps in enhancement. Any enhancement in convective heat transfer directly affects current energy production, as large scale energy production systems are reliant on convective fluid heat transfer. In this study, we investigated the potential use of nanoparticle colloids, as heat transfer enhancing coolants. New heat transfer fluids designed by scattering nanoparticles with a smaller average diameter than 100 nm (nanometer) in conventional heat transfer fluids are called nanofluids [1, 2]. The results of the recent studies show that the solid nanoparticles, suspended in the base fluid, with a high thermal conductivity enhance the convective heat transfer coefficient and the effective thermal conductivity of the base fluid [3-8]. However, more experimental and numerical analyses are needed to access a uniform approach.

The addition of nanoparticles to base fluids (traditional coolants: water, glycol and refrigerants) in order to improve their thermal conductivity and enhance the heat transfer performance was first demonstrated by Choi and Eastman [9]. Wang and Xu [10] showed that the addition of nanoparticles to liquid coolants increases the thermal conductivity and improves the overall cooling efficiency of the system. An excellent review of nanofluid physics and developments can be found in Refs. [11-13]. Many investigators such as Wen and Ding [14] measured heat transfer coefficients for various types of nanofluids. They found that the heat transfer coefficient increased with the increasing Reynolds number and particle volume concentration. Also, they observed the enhancement is particularly significant in the entrance region, and decreases with axial distance. Heris et al. [15] investigated laminar flow convective heat transfer of Al_2O_3-water and CuO-water nanofluids through circular tube with constant wall temperature boundary condition for the Reynolds numbers in the range of 700 to 2050. It was found that the Nusselt number is an increasing function of the Peclet number. It was also observed that the Nusselt number of nanofluids was always greater than the theoretical prediction and heat transfer rates. The achieved enhancement by using Al_2O_3-water which was higher than that of CuO-water. Anoop et al. [16] studied the effects of

*Corresponding author. Tel.: +98 611 3330010 (5678), Fax.: +98 611 3336642
E-mail address: a.r.noghrehabadi@scu.ac.ir
† Recommended by Associate Editor Dae Hee Lee

particle size on the convective heat transfer of alumina-water nanofluids. They found the nanofluid with 45 nm particles shows higher heat transfer coefficient than that with 150 nm particles. In addition, they observed that the enhancement of heat transfer coefficient in the developing region was higher than that in the developed region. Similar observations were reported by Esmaeilzadeh et al. [17] γ-Al_2O_3/water nanofluids. Experimental determination of heat transfer and pressure drop enhancement of low volume concentrations of Al_2O_3 nanofluids flowing in a tube and with inserted longitudinal strips has been undertaken by Sundar and Sharmag [18]. They observed that the enhancement in heat transfer in a plain tube with 0.5% volume concentration Al_2O_3 nanofluid (compared to water) were 17.36% and 30.30% for Reynolds numbers of 3000 and 22000. Kumar et al. [19] determined heat transfer coefficient and pressure drop of Al_2O_3 / water nanofluid with shell and helically coiled tube heat exchanger in the range of $5100 < Re < 8700$ and particle volume concentrations of 0.1%, 0.4% and 0.8%. The results indicated heat transfer coefficient enhancements of 18% and 25%, respectively, with particle volume concentration of 0.4% and 0.8%, compared to water.

There are several numerical studies about nanofluid convective heat transfer performance. Chamkha [20] numerically investigated the unsteady laminar flow and heat transfer of a particulate suspension in an electrically conducting fluid through channels and circular pipes in the presence of a uniform transverse magnetic field. Akbar [21] analyzed the effects of magnetic field on the flow and heat transfer of carbon nanotubes in a non-uniform tube. Shermet et al. [22] and Shermet and Pop [23] used the mathematical nanofluid model proposed by Buongiorno [24] to study of the steady free convection flow in shallow, slender and square porous cavities filled by a nanofluid. Noghrehabadi et al. [25] examined the effect of the partial slip boundary condition on the flow and thermal boundary layer of nanofluids over an isothermal stretching sheet. Influence of viscous dissipation and Newtonian heating on boundary layer flow of three types of water-based nanofluids containing metallic or nonmetallic nanoparticles over a flat plate was investigated by Makinde [26]. Zaraki et al. [27] theoretically analyzed the effect of the working temperature on the natural convective heat transfer of nanofluids over a flat plate. They found that the presence of nanoparticles reduces the efficiency of the nanofluid in heat removal. They pointed out that this is a crucial issue in real world application of nanofluid. The study of entropy generation is one of the major objectives in modeling and optimizing of energy systems, when it comes to find their optimum design condition. Noghrehabadi et al. [28] presented the effects of Brownian motion, thermophoresis and heat generation/absorption on entropy generation of a nanofluid over an isothermal linear stretching sheet with partial slip. Mkwizu and Makinde [29] investigated the entropy generation in an unsteady flow of water-based nanofluids confined between two parallel plates. The influence of Brownian motion and variable viscosity on entropy generation was evaluated. An analysis of entropy generation through plumb duct with peristalsis flow of carbon nanotube (CNT) suspension nanofluid is discussed by Akbar [30].

The convective heat transfer performance of Fe_3O_4/water magnetic nanofluids in the range of $3000 < Re < 22000$ and the volume concentration range of $0 < \phi < 0.6\%$ through a circular tube was studied experimentally by Sundar et al. [31]. They indicated that the enhancement of heat transfer coefficient in a plain tube with 0.6% volume concentration of Fe_3O_4 nanoparticles was 20.99% and 30.96% for Reynolds numbers of 3000 and 22000, respectively, compared to the base fluid. Rayatzadeh et al. [32] performed experiments to investigate the effect of adding TiO_2 nanoparticles to the distilled water on convective heat transfer with and without continuous induced ultrasonic field in the nanofluid's reservoir. The results indicated that about 5% increment in Nusselt numbers was observed in higher concentrations by continuous use of ultrasonic waves in comparison with the case with no sonication. Heat transfer enhancement capability of Al_2O_3-water nanofluids inside a circular tube in turbulent flow regimes was experimentally investigated by Sahin et al. [33]. The augmentation of the viscosity (due to presence of nanoparticles) was found to be more significant than the thermal conductivity of the nanofluids for the particle volume concentrations higher than 1 vol.%. Also, the highest heat transfer enhancement was achieved at $Re = 8000$ and 0.5 vol.%. Azmi et al. [34] reported an experimental work on the convective heat transfer of nanofluids, synthesized by SiO_2 nanoparticles and distilled water, flowing through a copper tube in the turbulent flow regime. The results showed enhancement of Nusselt number at 3.0% volume concentration in the Reynolds number range of 5000 and 27000 varied between 29% and 38%. Owing to the fact that nanofluids play important role in enhancement of thermal conductivity and heat transfer in fluid flows, in order to utilize nanofluids in conventional cooling applications, it is imperative to investigate convective heat transfer performance of nanofluids. However, a review of the literature shows that only a few studies have analyzed the Nusselt number of nanofluids in the developing regions, and hence, relations for calculating the Nusselt number of nanofluids in this region are highly demanded. The present study experimentally analyzes the laminar flow and convective heat transfer performance of γ-Al_2O_3/water nanofluids through a circular tube, subject to a uniform heat flux on its outside surface. New correlations are proposed for calculating Nusselt number in the developing region of the flow and heat transfer of nanofluids in tubes.

2. Preparation of nanofluid

There are two production methods for synthesizing nanofluids, one-step chemical methods and two-step methods. It has been demonstrated that the key to significant increment of thermal conductivity of nanofluids is the synthesis method, within which non-agglomerated nanoparticle are suspended in base fluid [35]. In one-step methods, preparing nanoparticles

Table 1. Specifications of nanoparticles.

Chemical formula	Al_2O_3
Morphology	Spherical
Crystal phase	Gamma
Mean diameter (nm)	20
Density (kg/m^3)	3890
Thermal conductivity (W/m K)	46
Specific heat (J/kg K)	880

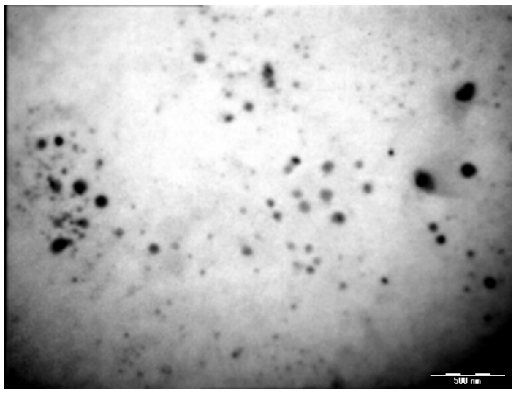

Fig. 1. TEM image of dispersed Al_2O_3 nanoparticles with an average diameter of 20 nm.

and dispersing them inside a base fluid occurs simultaneously. In two-step methods, nanoparticles are processed and made by some techniques first and then dispersed into a base fluid. In this study, nanofluid was prepared by dispersing Al_2O_3 nanoparticles in the deionized water as a base fluid by using the two-step method. The nanofluid was synthesized using the facilities of nanofluids laboratory by the researchers. Al_2O_3-γ (US Research Nanomaterials, Inc., USA) with a mean diameter of 20 nm nanoparticles were used. The physical properties, size and morphology of nanoparticles are shown in Table 1.

Fig. 1 shows the TEM (Transmission electron microscopy) image of Al_2O_3-γ nanoparticles used to synthesize the nanofluid. To investigate the effect of nanoparticle concentration, samples of nanofluids with volume concentrations of 0.1%, 0.3 and 0.9% were prepared by adding a specified amount of Al_2O_3 nanoparticles in deionized water. The nanoparticles were dispersed in the base fluid by aid of a mechanical stirrer (IKA RW 20 digital, Germany), then the suspensions were subjected to ultrasonic homogenizer (Hielscher UP400S, Germany) to provide a uniform dispersion and stable suspension. To reach proper stability of the nanofluids, the mechanical mixing and ultrasonic sonication were repeated several times. An image of the samples of nanofluids at different volume concentrations is shown in Fig. 2. No surfactant or pH changes were used as they may have some influence on the effective thermal conductivity of nanofluids [36]. The pH of the prepared nanofluid was measured by a pH meter (Metrohm 744, Switzerland) and found to be around 5, which was far from the isoelectric point of 9.2 for alumina nanoparticles [37]. This ensures the nanoparticles were well dispersed and the nanofluid was stable because of very large repulsive forces among the nanoparticles when pH was far from isoelectric point. Note that for each test a new nanofluid was prepared and utilized immediately to prevent any possible sedimentation. Also, no sedimentation was observed after 5 h.

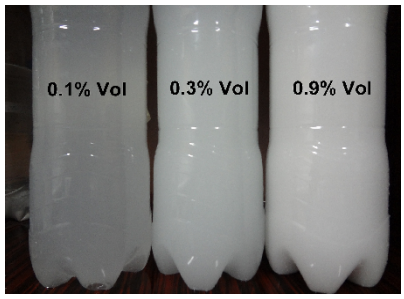

Fig. 2. Samples of prepared nanofluids at 0.1%, 0.3% and 0.9% volume concentration.

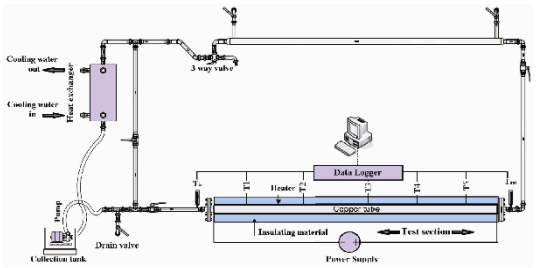

(a)

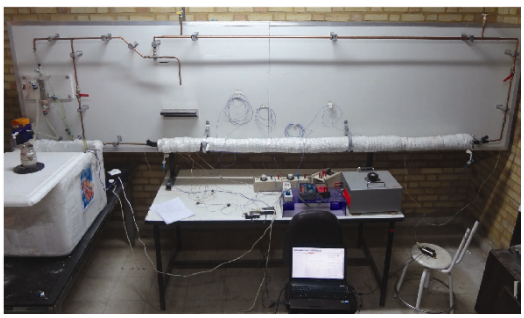

(b)

Fig. 3. (a) Schematic diagram; (b) view of the experimental setup.

3. Experimental setup

A schematic diagram and view of the experimental apparatus used to measure convective heat transfer coefficient is shown in Fig. 3. The setup consists of a copper heat transfer section, a cooling part, a pump, a power supply, a reservoir tank and a computer. The straight copper tube with 2.38 m length and 11.1 mm inner diameter was used as a test section. The thickness of the tube was measured as 1.6 mm. The whole section was electrically heated by 30 nichrome 20 wire (RESCALL, France) uniformly wound on the tube and connected to an AC power supply to generate constant heat.

Therefore, the heat flux could be adjusted by varying the voltage. The heat transfer section was isolated by 8 cm thick insulation consisting of a layer of ceramic fiber blanket and a layer of ceramic fiber rope at the outer surface to prevent radial heat loss to the surroundings. Additionally, the test section was thermally isolated from its upstream and downstream sections by Teflon flange with a length of 5 cm to avoid heat loss along the axial direction. Five K-type thermocouples (Class A, Testo Company, Germany) were mounted on the outer surface of the section at axial positions of 530 mm (T_{w1}), 830 mm (T_{w2}), 1130 mm (T_{w3}), 1562 mm (T_{w4}) and 1910 mm (T_{w5}) measured from the inlet of the section to probe the wall temperature. Two thermocouple probes (K-type) were inserted into the flow at the entrance and exit of the test section to measure the bulk temperatures of the nanofluid. The thermocouple measuring inlet temperature was located before a honeycomb to ensure the flow was not disturbed by the probe; the thermocouple measuring outlet temperature was located 10 cm away from the end of the test section and after the static mixture to prevent disturbing flow profiles in the test section and make a convenient measurement of the bulk mean temperature of fluid. The uncertainty in temperature measurements was ±0.1 °C. After the temperatures reached a steady state, data was collected from the thermocouples every 10 s by data loggers (176T4 and 175T3, Testo Company, Germany) connected to a computer. The flow rates were calculated by collecting the fluid in the collecting station with a precise measuring jar and stop watch (weight and time method). The fluid, after passing through the test section, flowed through the cooling unit, which was a shell and tube heat exchanger (HT33, Armfield, Inc., England) and finally was collected in a collecting tank. A counter-flow heat exchanger with a cold water supply and a pump (for circulation of the cold water in the heat exchanger) was used to take away heat from the nanofluid, which was absorbed in the test section. The heat exchanger facilitates temperature control of the nanofluid and keeps it constant at the inlet of the test section. Before the heat exchanger, a three-way valve was placed for cleaning the system between successive experimental runs. Two control valves and a bypass line were installed to help control the flow rate in the test section.

4. Data processing

The heat transfer performance of flowing nanofluids was defined in terms of the following convective heat transfer coefficient and the Nusselt number. The local Nusselt number and heat transfer coefficient are defined by:

$$Nu_{(x)} = \frac{h_{(x)}\, d_i}{k}, \tag{1}$$

$$h_{(x)} = \frac{q''}{T_{w(x)} - T_{f(x)}}, \tag{2}$$

where d_i is the tube inner diameter, k is the thermal conductivity of the test fluid, q'' is the heat flux, $T_{w(x)}$ is the wall temperature and $T_{f(x)}$ is the fluid bulk temperatures. From the energy balance equation, the bulk temperature of the fluid at an axial distance can be found by using:

$$T_{f(x)} = T_{f,i} + \frac{q'' P}{\dot{m} c_p} x, \tag{3}$$

where $T_{f,I}$, P, x, $\dot{m}$ and c_p are fluid bulk temperature at the inlet of the test section, perimeter of the copper tube, axial distance from the inlet of the test section, mass flow rate of the fluid and specific heat of the test fluid, respectively. In the heat transfer experiments, a uniform heat flux boundary condition was assumed on the channel wall. The wall heat flux was calculated using the energy balance as:

$$q'' = \frac{Q_1}{\pi d_i L}, \tag{4}$$

where L is the test section length, Q_1 is the energy supplied by the electrical heater. The energy supplied by the electrical heater was evaluated using the measured electrical current (I) and the supplied voltage (V) as:

$$Q_1 = I \times V \text{ (Energy supplied)}. \tag{5}$$

The absorbed energy by the nanofluid was also evaluated by using the following relation:

$$Q_2 = \dot{m} c_p (T_{f,o} - T_{f,i}) \text{(Energy absorbed)}, \tag{6}$$

where $T_{f,o}$ and $T_{f,i}$ are the fluid bulk temperatures at the outlet and inlet of the test section. $\dot{m}$ denotes the mass flow rate of the nanofluid in the test section. The maximum deviation between the electrical power input to the heater (estimated by Eq. (5)) and that absorbed by the testing fluid (evaluated by Eq. (6)) was less than 3.8%. This indicated that only a negligible amount of heat was lost from the test section into environment. For solid-liquid mixtures, the relative thermal conductivity can be estimated by the Maxwell model [38]. This model is applicable to statistically homogeneous and low volume fraction liquid-solid suspensions with randomly dispersed, uniformly sized and non-interacting spherical particles. The Maxwell equation is as follows:

$$\frac{k_{nf}}{k_f} = \frac{k_p + 2k_f + 2\phi(k_p - k_f)}{k_p + 2k_f - \phi(k_p - k_f)}, \tag{7}$$

where ϕ is the concentration of nanoparticles and k is the thermal conductivity. Properties with subscript ‘‘p” and ‘‘f” are for nanoparticles and base fluid, respectively. Density and specific heat of the nanofluids are estimated by Pak and Cho equation [39] and Xuan and Roetzel’s equation [40]. The density of nanofluid samples was evaluated based on the physical principle of the mixture rule. The specific heat of the nan-

ofluid samples was determined by considering thermal equilibrium between the nanoparticles and the base fluid phase. The density and specific heat of the nanofluid samples are evaluated using the following relations [39, 40]

$$\rho_{nf} = (1-\varphi)\rho_f + \varphi\rho_p \,, \tag{8}$$

$$(\rho C_p)_{nf} = (1-\varphi)(\rho C_p)_f + \varphi(\rho C_p)_p \,. \tag{9}$$

In this work, the Maiga equation [41] was used to estimate the viscosity of nanofluids as:

$$\mu_{nf} = (1 + 7.3\varphi + 123\varphi^2)\mu_f \,, \tag{10}$$

where μ_f is the viscosity of the base fluid. Eq. (10) was reported by Maiga et al. [41] and obtained by performing a least-square curve fitting on measured dynamic viscosity data of Al_2O_3-water. Note that the transport properties are functions of temperature. All the fluid thermo-physical properties are determined based on a mean bulk fluid temperature ($T_{f,b}$):

$$T_{f,b} = \frac{T_{f,o} + T_{f,i}}{2} \,. \tag{11}$$

The volume concentration is evaluated from the following relation:

$$\varphi = \frac{V_p}{V_p + V_f}, \qquad V_p = \frac{W_p}{\rho_p}, \quad V_f = \frac{W_f}{\rho_f} \,, \tag{12}$$

where W_p and W_f are the weights of the nanoparticles and water, respectively.

5. Uncertainty analysis

Uncertainty in the result of experiments depends on the square uncertainty of variables. The uncertainty of experimental results was estimated by using the proposed equation by Kline and McClintock [42]. For this purpose, quantities such as the tube diameter (d), length of the test section (L), axial distance from the inlet of the test section (x), mass flow rate ($\dot{m}$), voltage (V), current (I) and wall temperature (T_w) were measured and the probable errors in each of them were calculated to estimate the uncertainties associated with experimental data of convective heat transfer coefficient (see Appendix). The calculations indicate that the maximum and average of uncertainties in the reported experimental heat transfer coefficients is 4.1% and 2.7%, respectively.

6. Results and discussion

Before measuring the convective heat transfer coefficient of nanofluids, experiments were conducted with deionized water as the working fluid, to test the accuracy and reliability of the experimental setup. Two tests at Reynolds numbers of 1057 and 2131 were executed. Nusselt numbers along the axial length of the tube were calculated and plotted in Fig. 4. Shah [43-45] analyzed the flow and heat transfer of liquids in tubes and reported the following relation for the Nusselt number along a tube:

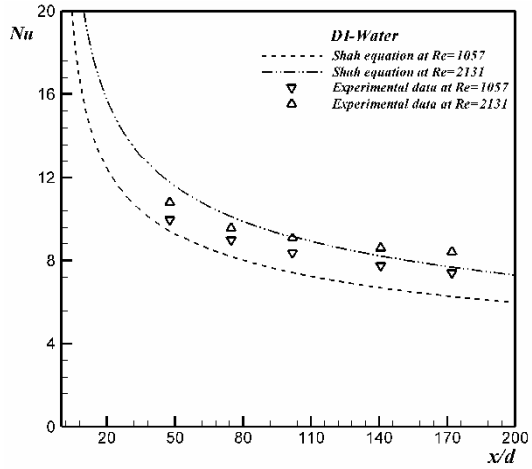

Fig. 4. Validation of the experimental setup at Re = 1057 and Re = 2131 for Nusselt number of DI-Water.

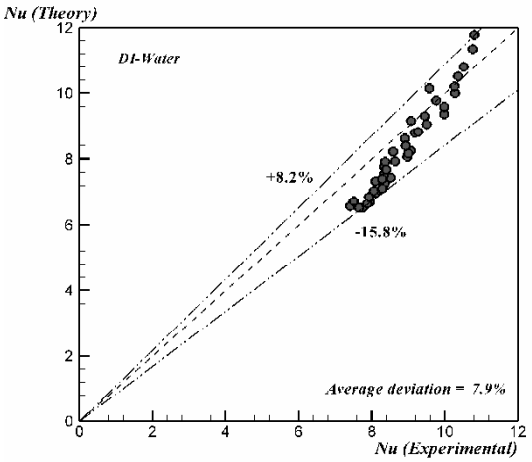

Fig. 5. Comparison between Shah equation and present experiment result for Nusselt number of DI-Water at Reynolds number between 1057 to 2130.

$$Nu = \begin{cases} 1.953(\mathrm{Re}\,\mathrm{Pr}\frac{d}{x})^{1/3} : \left(\mathrm{Re}\,\mathrm{Pr}\frac{d}{x}\right) \geq 33.3 \\ 4.364 + 0.0722\,\mathrm{Re}\,\mathrm{Pr}\frac{d}{x} : \left(\mathrm{Re}\,\mathrm{Pr}\frac{d}{x}\right) < 33.3 \end{cases} , \tag{13}$$

where Re is the Reynolds number and Pr is the Prandtl number. From Fig. 4, the experimental results are in good agreement with the predicted values. Fig. 5 presents the variation of theoretical values given by Eq. (13) with experimental values for local Nusselt number at different Reynolds numbers (1057, 1140, 1282, 1374, 1523, 1641, 1924 and 2131). As seen from

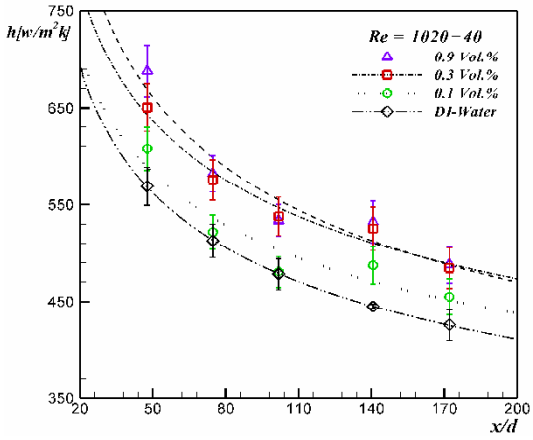

Fig. 6. Variation of convective heat transfer coefficient with respect to dimensionless axial length for different volume concentrations of nanofluid at Re = 1020.

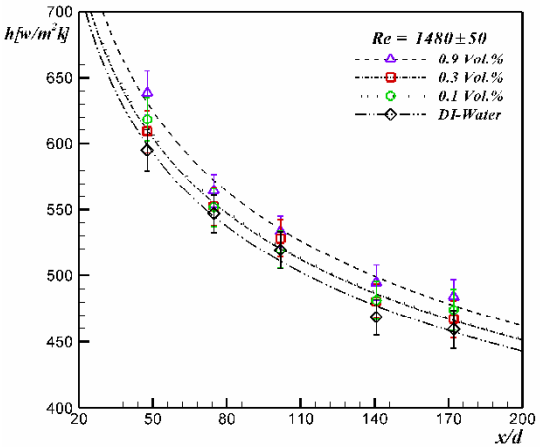

Fig. 7. Variation of convective heat transfer coefficient with respect to dimensionless axial length for different volume concentrations of nanofluid at Re = 1480.

this figure, the deviation of the experimental data from the theoretical one is within −15.8% and +8.2%. The deviation may be due to the differences in the size of the tubes. The Shah correlation was developed on the basis of laminar flows in large channels [46, 47], whereas a relatively small tube was considered in this study. Heat transfer tests were performed for the estimation of heat transfer coefficients for different volume fractions for Al_2O_3 (0.1%, 0.3% and 0.9%) and different Reynolds number approximately 1020, 1480 and 2070 at inlet temperature of 30°C with flow of deionized water and nanofluid. The error bars in Figs. 6-8 show the experimental uncertainty in the heat transfer coefficient, which is calculated in the Appendix. The local heat transfer coefficients measured at five axial distances T_{w1} to T_{w5} for different volume fractions are presented in Fig. 6 when Re = 1020. The local heat transfer coefficient of nanofluids was observed to be enhanced as compared to the base fluid. The local heat transfer coefficient increases with increasing particle volume concentration. As an example, at the 0.9% volume concentration, the heat transfer coefficient of nanofluids was approximately 18% greater than the base fluid at x/d = 47.74. As investigated before, the addition of nanoparticles enhances the thermal conductivity of the base fluid. This enhancement in thermal conductivity would increase the convective heat transfer coefficient. The variation of convective heat transfer coefficient with respect to dimensionless axial length for different volume concentrations of nanofluid at Re = 1480 is depicted in Fig. 7. It is evident that the local heat transfer coefficients decreases with increasing dimensionless axial length. Fig. 8 shows the variation of convective heat transfer coefficient with respect to dimensionless axial length for different volume concentrations of nanofluid at Re = 2070. From Fig. 8, the maximum heat transfer coefficient increase of about 23% is achieved x/d = 47.74 when nanofluid with 0.9% volume concentration is used. Also, the enhancement is also more at the entrance region than at a higher x/d. Fig. 9 illustrates the ratio of experimental convective heat transfer coefficient of nanofluid at 0.9% volume con-

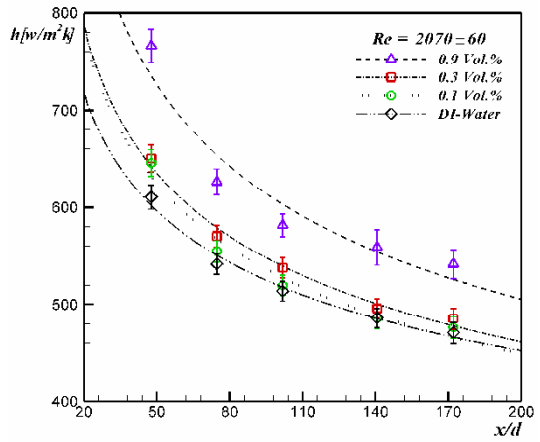

Fig. 8. Variation of convective heat transfer coefficient with respect to dimensionless axial length for different volume concentrations of nanofluid at Re = 2070.

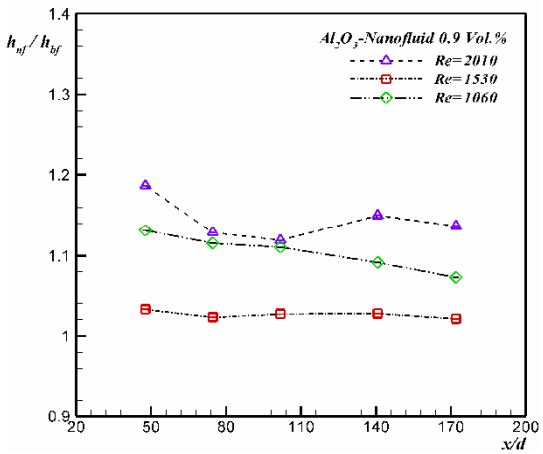

Fig. 9. The ratio of experimental convective heat transfer coefficient of nanofluid (0.9 Vol.%) to that of DI-Water versus dimensionless axial length at different Reynolds number.

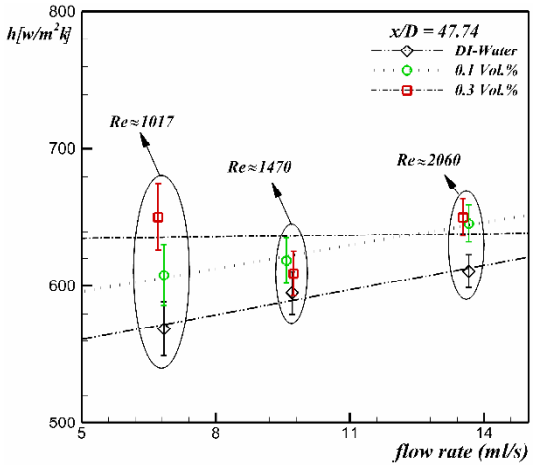

Fig. 10. Variation of convective heat transfer coefficient with respect to flow rate at position 1 (x/d = 47.74).

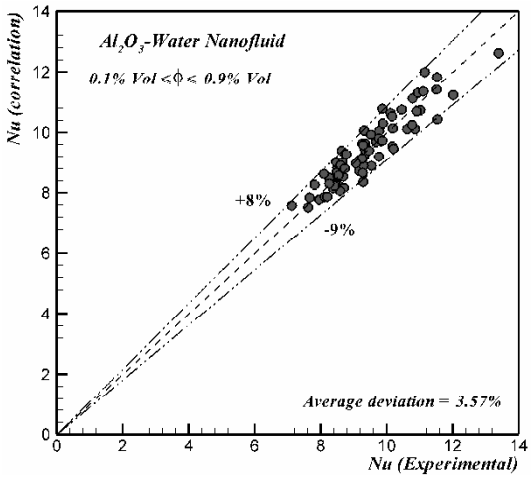

Fig. 11. Comparison of the Nusselt number of nanofluids between predicted values by presented correlation and experimental data.

centration to that of deionized water as a function of dimensionless axial length in different Reynolds number. Also from Fig. 9, the maximum enhancement ratio occurred at the highest Reynolds number (2010) of nanofluid at 0.9% volume concentration. Variations of convective heat transfer coefficient with nanofluid flow rate (velocity profiles) at x/d = 47.74 are illustrated in Fig. 10. Based on these results, the addition of nanoparticles results in an enhancement of the convective coefficient of a base fluid (water). It is clear that the presence of nanoparticles increases the thermal conductivity of the fluid, and consequently results in enhancement of the convective heat transfer. Therefore, the migration of nanoparticles due to a possible mechanism such as thermophoresis, Brownian motion and shear lift force, resulting in redistribution of nanoparticles in the tube, can be significant. The thermophoresis force tends to move the particles from the vicinity of the tube wall (hot regions) into the core of the tube. In contrast, Brownian motion tends to make uniform the nanoparticles in the tube. The migration of nanoparticles affects the hydrodynamic velocity profiles as well as the temperature distribution in the cross-section of the tube. When the flow rate is low, the migration mechanism is more effective because there might be sufficient time for the migration and redistribution of nanoparticles in the tube. As the flow rate increases, the nanofluid would pass through the tube more quickly, and hence, the nanoparticles may have not enough time to properly redistribute in the cross-section of the tube. The lack of radial migration may explain the lack of heat transfer increase at Re = 1530 in Fig. 9. According to this figure, convective heat transfer coefficient for 0.9% volume concentration suddenly jumped to a higher value. This could be due to occurrence of the transient from laminar to turbulent, which significantly increased the convective heat transfer despite nanoparticle migration mechanisms. The experimental results were used to develop an empirical correlation for local Nusselt number and local heat transfer coefficient for Al_2O_3 /water nanofluid in the case of laminar flow through circular tube. This is one of the

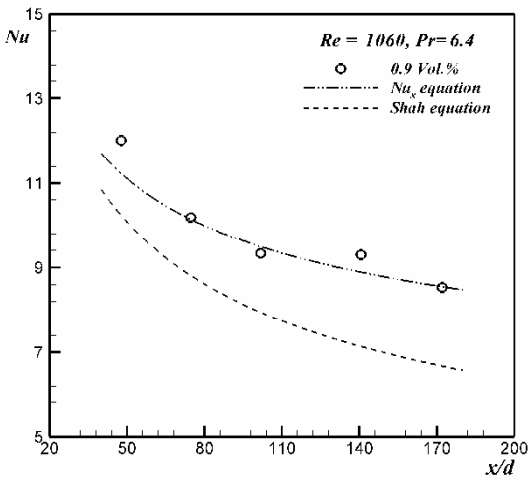

Fig. 12. Deviation between measured data and the values of Nusselt number of nanofluid calculated by Shah equation and presented correlation at 0.9% volume concentration.

important issues in this study. In general, local Nusselt numbers and local heat transfer coefficient of nanofluids may be related to the parameters as follows:

$$Nu_{(x)} = f(\mathrm{Re}_{nf}, \mathrm{Pr}_{nf}, \phi, \frac{d}{x}), \tag{14}$$

$$h_{(x)} = \frac{Nu_{(x)} \times k_{nf}}{d}. \tag{15}$$

Considering the above mentioned, the correlation for predicting the heat transfer performance of nanofluid was formed and is proposed in the following form:

$$Nu_{(x)} = 4.36 + (3 + \phi^{0.442})\,\mathrm{Re}_{nf}^{\;0.288}\,\mathrm{Pr}_{nf}^{\;0.0185}\left(\frac{d}{x}\right)^{0.3851}. \tag{16}$$

The above equation is obtained by curve fitting all the experimental data for the nanofluids. These correlations are valid

for Al_2O_3 /water nanofluid flow with volume concentration 0.1% through 0.9% in developing region $40 < x/d < 180$ for laminar flow regime with $900 < Re < 2100$. Fig. 11 shows a comparison of the Nusselt number of nanofluids between predicted values by presented correlation and experimental data. This figure shows that the deviation of experimental data and empirical correlation, which is in the range of -9% to +8%. Fig. 12 also shows the deviation between measured data and the values of Nusselt number of nanofluid calculated by Shah equation and presented correlation with 0.9% volume concentration at Reynolds number of 1060. From this figure, the measured Nusselt number for nanofluids is higher than that for water, and the Shah equation fails to predict the measured results.

7. Conclusion

The convective heat transfer characteristics of Al_2O_3 /water nanofluids flowing through a circular tube in laminar flow regime were studied experimentally. Following conclusions are presented based on the experimental results:

- Al_2O_3 /water nanofluid enhances heat transfer compared with base fluid.
- Increasing the nanoparticle concentrations of Al_2O_3 /water nanofluid increases the convection heat transfer enhancement of nanofluid. The maximum percentage enhancement in convection heat transfer was 22.5%, and was observed with 0.9% volume concentration.
- The maximum enhancement is particularly significant at lower *x/d* ratios. The results of local heat transfer coefficient evaluated for various *x/d* are useful in order to optimize the length of the tube or heat exchanger for maximum heat transfer. It is suggested that the nanofluid has potential to be applied within the thermally developing region when utilizing the nanofluid as a heat transfer liquid in a circular tube.
- The convective heat transfer coefficient of Al_2O_3 /water nanofluids is increased with volume concentration of Al_2O_3 nanoparticles, but cannot be predicted by Shah equation. Therefore, a new empirical correlation is developed for Al_2O_3 /water nanofluid local Nusselt number with mean deviation of 3.57% from the experimental data.

Acknowledgements

The authors acknowledge Shahid Chamran University of Ahvaz and Iran Nanotechnology Initiative Council (INIC) for the financial supports of this research.

Nomenclature

A : Tube cross-sectional area
D : Tube diameter
C_p : Heat capacity of the fluid
h : Heat transfer coefficient
I : Current
K : Thermal conductivity
$\dot{m}$: Mass flow rate
Nu : Nusselt number
P : Perimeter of tube
Pr : Prandtl number
Q : Heat flow
q'' : Heat flux
Re : Reynolds number
T_f : Fluid bulk temperature
T_w : Temperature at the tube
V : Voltage
x : Axial distance

Greek

μ : Viscosity
ρ : Density
φ : Nanoparticle volume fraction

Subscripts

nf : Nanofluid
f : Base fluid
p : Nano-particles
in : Inlet
out : Outlet

References

[1] W. W. Duangthongsuk and S. B. Wongwises, Comparison of the effects of measured and computed thermo-physical properties of nanofluids on heat transfer performance, *Exp. Therm. Fluid. Sci*., 34 (2010) 616-624.
[2] J. H. Lee, K. S. Hwang, S. P. Jang, B. H. Lee, J. H. Kim, S. U. S. Choi and C. J. Choi, Effective viscosities and thermal conductivities of aqueous nanofluids containing low volume concentrations of Al_2O_3 nanoparticles, *Int. J. Heat Mass Transf.,* 51 (2008) 2651-2656.
[3] S. U. S. Choi, Enhancing thermal conductivity of fluids with nanoparticles, *ASME FED*, 231 (1995) 99-105.
[4] J. A. Eastman, S. U. S. Choi, S. Li, W. Yu and L. J. Thompson, Anomalously increased effective thermal conductivities of ethylene glycol based nanofluids containing copper nanoparticles, *Appl. Phys. Lett*., 78 (2001) 718-720.
[5] S. Lee, S. U. S. Choi, S. Li and J. A. Eastman, Measuring thermal conductivity of fluids containing oxide nanoparticles, *J. Heat Transf*., 121 (1999) 280-289.
[6] Y. M. Xuan and Q. Li, Heat transfer enhancement of nanofluids, *Int. J. Heat. Fluid. Flow,* 21 (2000) 58-64.
[7] H. Xie, J. Wang, T. G. Xie, Y. Liu and F. Ai, Thermal conductivity enhancement of suspensions containing nanosized alumina particles, *J. Appl. Phys*., 91 (2002) 4568-4572.
[8] S. K. Das, S. U. S. Choi and H. E. Patel, Heat transfer in

nanofluids-a review, *Heat. Transf. Eng*., 37 (2006) 3-19.

[9] S. Choi and J. A. Eastman, Enhancing thermal conductivity of fluids with nanoparticles, *ASME Int. Mech. Eng. Congr. Expos*., San Francisco, CA (1995) 99-105.

[10] X. W. Wang and X. F. Xu, Thermal conductivity of nanoparticle-fluid mixture, *J. Thermophys. Heat. Transf*., 13 (1999) 474-480.

[11] W. Daungthongsuk and S. Wongwises, A critical review of convective heat transfer nanofluids, *Renew. Sustain. Energy Rev*., 11 (2007) 797-817.

[12] V. Trisaksri and S. Wongwises, Critical review of heat transfer characteristics of nanofluids, *Renew. Sustain. Energy Rev*., 11 (2007) 512-523.

[13] M. Chandrasekar, S. Suresh and T. Senthilkumar, Mechanisms proposed through experimental investigations on thermophysical properties and forced convective heat transfer characteristics of various nanofluids - A review, *Renew. Sustain. Energy Rev*., 16 (2012) 3917-3938.

[14] D. Wen and Y. Ding, Experimental investigation into convective heat transfer of nanofluids at the entrance region under laminar flow conditions, *Int. J. Heat. Mass. Transf*., 47 (2004) 5181-5188.

[15] S. Z. Heris, S. Gh. Etemad and M. N. Esfahany, Experimental investigation of oxide nanofluids laminar flow convective heat transfer, *Int. Commun. Heat. Mass. Transf*., 33 (2006) 529-535.

[16] K. B. Anoop, T. Sundararajan and S. K. Das, Effect of particle size on the convective heat transfer in nanofluid in the developing region, *Int. J. Heat. Mass. Transf*., 52 (2009) 2189-2195.

[17] E. Esmaeilzadeh, H. Almohammadi, Sh. N. Vatan and A. N. Omrani, Experimental investigation of hydrodynamics and heat transfer characteristics of γ-Al_2O_3/water under laminar flow inside a horizontal tube, *Int. J. of Therm. Sci*., 63 (2013) 31-37.

[18] L. S. Sundar and K. V. Sharma, Heat transfer enhancements of low volume concentration Al_2O_3 nanofluid and with longitudinal strip inserts in a circular tube, *Int. J. Heat. Mass. Transf.,* 53 (2010) 4280-4286.

[19] P. C. Mukesh Kumar, J. Kumar and S. Suresh, Experimental investigation on convective heat transfer and friction factor in a helically coiled tube with Al_2O_3/water nanofluid, *J. Mech. Sci. Technol.,* 27 (2013) 239-245.

[20] A. J. Chamkha, Unsteady laminar hydromagnetic fluid-particle flow and heat transfer in channels and circular pipes, *Int. J. Heat Fluid Flow,* 21 (6) (2000) 740-746.

[21] N. Akbar, Heat transfer and carbon nano tubes analysis for the peristaltic flow in a diverging tube, *Meccanica,* 50 (2015) 39-47.

[22] M. A. Sheremet, T. Groşan and I. Pop, Free convection in shallow and slender porous cavities filled by a nanofluid using Buongiorno's model, *J. Heat. Transf.,* 136 (2014) 082501.

[23] M. A. Sheremet and I. Pop, Conjugate natural convection in a square porous cavity filled by a nanofluid using Buongiorno's mathematical model, *Int. J. Heat Mass Transf*., 79 (2014) 137-145.

[24] J. Buongiorno, Convective transport in nanofluids, *ASME J. Heat Transf.,* 128 (2006) 240-250.

[25] A. Noghrehabadi, R. Pourrajab and M. Ghalambaz, Effect of partial slip boundary condition on the flow and heat transfer of nanofluids past stretching sheet prescribed constant wall temperature, *Int. J. Thermal Sci*., 54 (2012) 253-261.

[26] O. D. Makinde, Effects of viscous dissipation and Newtonian heating on boundary-layer flow of nanofluids over a flat plate, *Int. J. Numer. Methods. Heat. & Fluid. Flow,* 23 (2013) 1291-1303.

[27] A. Zaraki, M. Ghalambaz, A. J. Chamkha, M. Ghalambaz and D. D. Rossi, Theoretical analysis of natural convection boundary layer heat and mass transfer of nanofluids: Effects of size, shapen and type of nanoparticles, type of base fluid and working temperature, *Adv. Powder. Technol*. (2015) doi:10.1016/j.apt.2015.03.012.

[28] A. Noghrehabadi, M. Saffarian, R. Pourrajab and M. Ghalambaz, Entropy analysis for nanofluid flow over a stretching sheet in the presence of heat generation/absorption and partial slip, *J. Mech. Sci. Technol*., 27 (2013) 927-937.

[29] M. H. Mkwizu and O. D. Makinde, Entropy generation in a variable viscosity channel flow of nanofluids with convective cooling, *Comptes Rendus Mécanique,* 343 (2015) 38-56.

[30] N. Akbar, Entropy generation analysis for a CNT suspension nanofluid in plumb ducts with peristalsis, *Entropy,* 17 (2015) 1411-1424.

[31] L. S. Sundar, M. T. Naik, K. V. Sharma, M. K. Singh and T. Ch. S. Reddy, Experimental investigation of forced convection heat transfer and friction factor in a tube with Fe_3O_4 magnetic nanofluid, *Exp. Therm. Fluid. Sci*., 37 (2012) 65-71.

[32] H. R. Rayatzadeh, M. Saffar-Avval, M. Mansourkiaei and A. Abbassi, Effects of continuous sonication on laminar convective heat transfer inside a tube using water-TiO_2 nanofluid, *Exp. Therm. Fluid. Sci*., 48 (2013) 8-14.

[33] B. Sahin, G. G. Gültekin, E. Manay and S. Karagoz, Experimental investigation of heat transfer and pressure drop characteristics of Al_2O_3-water nanofluid, *Exp. Therm. Fluid. Sci*., 50 (2013) 21-28.

[34] W. H. Azmi, K. V. Sharma, P. K. Sarma, R. Mamat, S. Anuar and V. D. Rao, Experimental determination of turbulent forced convection heat transfer and friction factor with SiO_2 nanofluid, *Exp. Therm. Fluid. Sci*., 51 (2013) 103-111.

[35] S. K. Das, S. U. S. Choi, W. Yu and T. Pradeep, *Nanofluids, Science and technology*, Wiley (2008).

[36] S. K. Das, N. Putra, P. Thiesen and W. Roetzel, Temperature dependence of thermal conductivity enhancement for nanofluids, *J. Heat. Transf*., 125 (2003) 567-574.

[37] H. Xie, L. Chen and Q. Wu, Measurements of the viscosity of suspensions (nanofluids) containing nanosized Al_2O_3 particles, *High Temperatures - High Pressures,* 37 (2008) 127-135.

[38] J. C. Maxwell, *A treatise on electricity and magnetism*,

Second ed., Clarendon Press, Oxford, UK (1881).
[39] B. Pak and Y. Cho, Hydrodynamic and heat transfer study of dispersed fluids with submicron metallic oxide particles, *Exp. Heat Transf.*, 11 (1998) 151-170.
[40] Y. Xuan and W. Roetzel, Conceptions for heat transfer correlation of nanofluids, *Int. J. Heat. Mass. Transf.*, 43 (2000) 3701-3707.
[41] S. E. B. Maïga, S. J. Palm, C. T. Nguyen, G. Roy and N. Galanis, Heat transfer enhancement by using nanofluids in forced convection flows, *Int. J. Heat. Fluid. Flow.*, 26 (2005) 530-546.
[42] J. Kline and F. A. McClintock, Describing uncertainties in single sample experiments, *Mech. Eng.*, 75 (1953) 3-8.
[43] R. K. Shah, Thermal entry length solutions for the circular tube and parallel plates, *Proc. of Third National Heat. Mass. Transfer*, Bombay (1975).
[44] R. K. Shah and A. L. London, *Laminar flow forced convection in ducts*, New York: Supplement 1 to Advances in heat transfer, Academic Press (1978).
[45] R. K. Shah and M. S. Bhatti, Laminar convective heat transfer in ducts, in: S. Kakaç, R. K. Shah and W. Aung (Eds), *Handbook of single-phase convective heat transfer*, Wiley, New York (1987).
[46] G. P. Celata, M. Cumo and G. Zummo, Thermal-hydraulic characteristics of single phase flow in capillary pipes, *Exp. Therm. Fluids Sci.,* 28 (2004) 87-95.
[47] Z. Y. Guo and Z. X. Li, Size effect on single-phase channel flow and heat transfer at microscale, *Int. J. Heat Fluid Flow,* 24 (2003) 284-329.

Appendix

The details for evaluating the uncertainty of the heat transfer coefficient measurements are described in this section. Heat transfer coefficient is defined from the Newton law of cooling as:

$$h = \frac{q''}{T_w - T_b} . \tag{A.1}$$

The uncertainty of Eq. (A.1), can be written as follows:

$$\delta h = \sqrt{\left(\frac{\partial h}{\partial q''}\delta q''\right)^2 + \left(\frac{\partial h}{\partial T_w}\delta T_w\right)^2 + \left(\frac{\partial h}{\partial T_b}\delta T_b\right)^2} . \tag{A.2}$$

However, to evaluate Eq. (A.1), the uncertainties of the heat flux ($\delta q''$) and temperatures (δT_w, δT_b) are required. The heat flux is determined by:

$$q'' = \frac{I\,V}{\pi\, d_i\, L} . \tag{A.3}$$

The uncertainty equation for the heat flux Eq. (A.3), is:

$$\delta q'' = \sqrt{\left(\frac{\partial q''}{\partial I}\delta I\right)^2 + \left(\frac{\partial q''}{\partial V}\delta V\right)^2 + \left(\frac{\partial q''}{\partial d_i}\delta d_i\right)^2 + \left(\frac{\partial q''}{\partial L}\delta L\right)^2} . \tag{A.4}$$

Bulk fluid temperature is calculated by the following equation:

$$T_b = T_{b,i} + \frac{q''\,\pi\, d_i\, x}{\rho\, Q\, c_p} . \tag{A.5}$$

The uncertainty of Eq. (A.5), can be evaluated as follows:

$$\delta T_b = \sqrt{\left(\frac{\partial T_b}{\partial q''}\delta q''\right) + \left(\frac{\partial T_b}{\partial \rho}\delta \rho\right) + \left(\frac{\partial T_b}{\partial Q}\delta Q\right) + \left(\frac{\partial T_b}{\partial c_p}\delta c_p\right) + \left(\frac{\partial T_b}{\partial x}\delta x\right) + \left(\frac{\partial T_b}{\partial d_i}\delta d_i\right) + \left(\frac{\partial T_b}{\partial T_{b,i}}\delta T_{b,i}\right)} . \tag{A.6}$$

The volumetric flow rate is obtained by:

$$Q = \frac{ml}{S} \times 10^{-6} , \tag{A.7}$$

where *ml* is the volume of the flow that measured in the specific time (*S*). The uncertainty for the volumetric flow rate Eq. (A.7), is found to be:

$$\delta Q = \sqrt{\left(\frac{\partial Q}{\partial S}\delta S\right)^2 + \left(\frac{\partial Q}{\partial ml}\delta ml\right)^2} . \tag{A.8}$$

Eqs. (A.1)-(A.8) are solved by using MAPLE where the heat transfer coefficient uncertainty is obtained.

Aminreza Noghrehabadi is an associate professor in Mechanical Engineering at Shahid Chamran University of Ahvaz. His research interests are on the field of nanofluid heat and mass transfer, NEMS actuators and heat transfer in porous media.

Rashid Pourrajab is graduate M.S. in Mechanical Engineering at Shahid Chamran University of Ahvaz. His research has been mainly focused on the development of new heat transfer enhancement fluid called nanofluids. He is working on modeling, production and experiments with nanofluids.